# Chapter 5

# Flow in an expanding channel

## 5.1 Preface

In this section, we introduce some further developments of the method of averaging. Our final goal is to describe the bifurcation leading to wave-breaking in the circular hydraulic jump. There is a close connection between the symmetric flows in a symmetric channel and a boundary layer flow with a free surface. In a two-dimensional boundary layer flow with a free surface, the shear-stress condition on the free surface in the boundary layer approximation is given by

$$\frac{\partial u}{\partial y}\Big|_{y=h(x)} = 0 \ , \tag{5.1}$$

where $u$ is the $x$-component of the velocity. It has been known for a long time [2] that the boundary layer equations (1.15) are invariant with respect to deformation of the boundary $y \to y + d(x)$, where $d(x)$ is an arbitrary function of $x$. If we chose $d(x) = -h(x)$, then the bottom $y = 0$ will transform to $y = -h(x)$, and the top $y = h(x)$ will transform to $y = 0$. Since the derivative with respect to $y$ of the velocity at the surface vanishes, we can 'flip' the picture about the $y = 0$ axis and get a flow which is symmetric and smooth around $y = 0$. For such a flow, the fluid is contained between rigid surfaces situated at $y = h(x)$ and $y = -h(x)$, as shown in figure 5.1. That is the reason why we have examined the problem of a symmetry-breaking bifurcation in a symmetric channel.

The flow is two-dimensional, and the fluid is flowing between walls situated at $y = h(x)$ and $y = -h(x)$, as shown in figure 5.1. For low Reynolds numbers $R$, the velocity field is symmetric with respect to the reflection $y \to -y$. If the Reynolds number is increased, a series of symmetry-breaking bifurcations occurs. These bifurcations have been studied theoretically in [1], [2] and experimentally in [3].

The flow in such a channel is described by the Navier-Stokes equations:

$$\begin{aligned} &u_t + uu_x + wu_y = -p_x + \frac{1}{R}\Delta u \\ &w_t + uw_x + ww_y = -p_y + \frac{1}{R}\Delta w \\ &u_x + w_y = 0, \end{aligned} \tag{5.2}$$

where $u$ and $w$ are the velocity components in $x$ and $y$ directions respectively, $p$ is the pressure and $\Delta = \partial_x^2 + \partial_y^2$ is the Laplace operator. If the mass flux into the channel is $2Q$

and the viscosity of the fluid is $\nu$, the Reynolds number $R$ in (5.2) equals $R = Q/\nu$. If we define the streamfunction $\psi$ as

$$u = \psi_y \qquad w = -\psi_x, \tag{5.3}$$

the system (5.2) can be rewritten as a single equation for the streamfunction $\psi$:

$$\Delta\psi_t + J(\Delta\psi, \psi) = \frac{1}{R}\Delta\Delta\psi, \tag{5.4}$$

where $J$ is the 'Jacobian' of two functions: $J(f,g) = f_x g_y - f_y g_x$. The streamfunction $\psi$ must satisfy the following boundary conditions:

$$\begin{aligned} &\psi(y = \pm h(x)) = \pm 1 \\ &\psi_y(y = \pm h(x)) = 0. \end{aligned} \tag{5.5}$$

The first condition of (5.5) specifies the conservation of mass flux in the channel, since the total flux equals to $\psi(y = h(x)) - \psi(y = -h(x)) = 2$. The no-slip condition $u = w = 0$ on the boundary follows from (5.5).

In what follows, we shall use the boundary layer approximation of (5.4). We shall assume that the channel is very thin and that the typical rate of change in the $y$ direction is much larger than the typical rate of change in the $x$ direction. In this approximation, (5.2) simplifies to:

$$\psi_{yyt} + J(\psi_{yy}, \psi) = \frac{1}{R}\psi_{yyyy}. \tag{5.6}$$

The boundary conditions (5.5) are unchanged.

In [1], the bifurcations were analysed by directly solving (5.2)-(5.5) on a computer using a finite-difference scheme. We shall develop simplified models of (5.2)-(5.5) and compare the results, provided by these models, with these of [1], as well as with simulations of the full Navier-Stokes equations, which were provided to us by K. H. Andersen. Our goal will be twofold. First, we would like to make a model which describes the symmetric solution accurately. Second, we would like to predict the symmetry breaking bifurcation. First, we develop the *minimal error method*. The essence of this method is to take a larger number of integrated boundary layer momentum equations than the number of unknowns, and then to minimise the error we make by choosing a particular solution. This trick allows us to compute the symmetric solutions quickly and quite accurately, even if the separation occurs. Unfortunately, no symmetry-breaking bifurcations were observed. The second way is to go beyond the boundary layer approximations and to include extra terms from the full Navier Stokes equations, which were neglected in the boundary layer approximations (*extended boundary layer method*). This method allows us to describe the symmetry-breaking bifurcation accurately.

We shall start this chapter with an explanation of why the integral methods need correction.

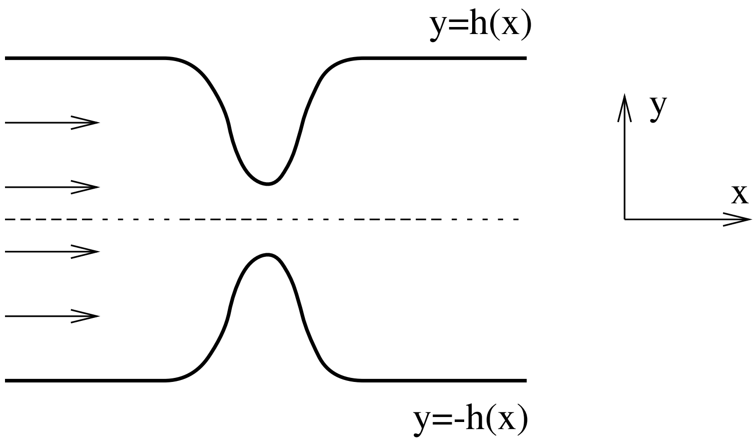


Figure 5.1: Flow in a symmetric channel. If the Reynolds number of the flow is increased, the flow ceases to be symmetric.

## 5.2 Singularities of the integral method

As we have seen in previous chapters, the integral (averaging) method works reasonably well provided that the solution of (2.42) does not reach the value $\Lambda = 0$. Close to this singular value $\Lambda = 0$, all the trajectories have a singularity of the type $\Lambda \simeq (r_0 - r)^{1/2}$. The singularity at $\Lambda = 0$ means that the values with $\Lambda > 0$ are unattainable, if we start with the values $\Lambda < 0$. This puts severe constraints on the behaviour of the solution: for example, the top velocity cannot become negative and, thus, a roller cannot be formed. In fact, the top velocity is $v(a+b+c)$, where $v$ is the average velocity, and $a, b, c$ are given by (2.38). Since the top velocity is negative when $a+b+c = -\Lambda/6 + 11/12 < 0$, we have $\Lambda > 11/2$.

Artificial singularities of the type $\Lambda = 0$ are a general drawback of averaged models. We shall illustrate this for the problem of the flow in a symmetric channel described above. Suppose that we try to approximate the solution $\psi$ of (5.2) by an $N+3$-th parameter profile, for example:

$$\psi(x, \eta) = \sum_{k=0}^{N+2} a_k(x)\eta^k, \tag{5.7}$$

where $\eta = z/h(x)$. The boundary conditions (5.5) give 4 linear equations for the functions $a_0(x), a_1(x), \ldots, a_{N+2}(x)$:

$$\begin{aligned} &\textstyle\sum_{k=0}^{N+2} a_k(x) = 1 \\ &\textstyle\sum_{k=0}^{N+2} (-1)^k a_k(x) = 1 \\ &\textstyle\sum_{k=1}^{N+2} k a_k(x) = 0 \\ &\textstyle\sum_{k=1}^{N+2} (-1)^k k a_k(x) = 0. \end{aligned} \tag{5.8}$$

For example, the three last coefficients $a_N(x), a_{N+1}(x), a_{N+2}(x)$ can be expressed in terms of the other $N$ variables $a_0(x), a_1(x), \ldots, a_{N-1}(x)$ from (5.8). Since we have $N$ unknowns, we have to write $N$ integrated momentum equations to make the resulting system well-defined. This can be done by multiplying the equation of motion by a weight function $I_m(y)$ (for example, by $I_m(y) = u(x,y)^{(m-1)}$) and integrating with respect to $y$ from $-h(x)$ to $h(x)$. Then, equation number $m$ will have the form

$$\sum_{k=1}^{n} F_{km}(\boldsymbol{a},x)a'_k + G_m(\boldsymbol{a},\boldsymbol{a}',x) = 0. \tag{5.9}$$

Equations (5.9) form a differential system for the vector $\boldsymbol{a}(x) = (a_0(x),\ldots,a_{N-1}(x))$, which can be written in a matrix form as

$$\boldsymbol{F}(\boldsymbol{a},x)\boldsymbol{a}' + \boldsymbol{G}(\boldsymbol{a},x) = 0, \tag{5.10}$$

where $\boldsymbol{F}$ and $\boldsymbol{G}$ are $N \times N$ matrices. The system (5.10) is solvable for the derivative $\boldsymbol{a}'$ if the determinant of the matrix $F$ is non-zero. Thus, the condition $\det \boldsymbol{F}(\boldsymbol{a},x) = 0$ specifies a singular surface of codimension 1 in an $N$-dimensional phase space. Because of this singular surface, it is impossible for the solution to reach regions of phase space isolated by $\det \boldsymbol{F}(\boldsymbol{a},x) = 0$, like the domain $\Lambda > 0$ in the system (2.42).

We have designed two methods of dealing with this problem, as we have already mentioned. The first one, the error minimisation method, is a trick designed to remove the singularity $\det \boldsymbol{F}(\boldsymbol{a},x) = 0$. In this method we remain fully in the boundary layer approximation (5.6), but we learn how to make effective use of the integrated momentum equations. The second method is, in a sense, more physical: it takes into account terms neglected in the boundary layer equation (5.6), and we thus call this method the extended boundary layer method. The rest of this chapter will be devoted to the description of these methods.

## 5.3 Error minimisation method

The singularity $\det \boldsymbol{F} = 0$ in (5.10) is unphysical. It comes from the fact that at the singular point $\boldsymbol{a}_*$ and $x_*$ the chosen basis $\left\{1,\eta,\eta^2,\ldots,\eta^N\right\}$ becomes degenerate. If we chose a different basis, say, $\{P_1(\eta),\ldots,P_N(\eta)\}$, the solution will be regular at the point $\boldsymbol{a}_*, x_*$, but it will be singular at another point of the phase space. One can draw a geometrical analogy with the covering of manifolds by local coordinate charts. Often, one cannot cover the whole manifold *globally* by the same coordinate chart without singularities, but several *local* coordinate charts can describe the whole manifold. On our case, a single basis is not sufficient for describing the solution everywhere, but a different basis can describe the solution where the first basis encounters trouble. This is an intuitive picture, but the question is how to formalise it?

We propose the following way of solving this problem. Suppose we consider an $N$-parameter profile for the velocity (5.7). Then, we have to use exactly $N$ equations for the expansion coefficients $a_k(x)$. However, our expansion (5.7) is only an approximation to the solution. Thus, when we use the exact equations of the type (5.10), we encounter the difficulty $\det \boldsymbol{F} = 0$ since we are attempting to substitute an approximate ansatz into the exact equations. One should thus consider (5.10) as being only an approximate equation, which the solution does not have to satisfy exactly.

There is a certain freedom in choosing the integration weights $I_m(z)$ used to obtain equation (5.10). Suppose we had chosen another weight $I_N(z)$ for the last equation of (5.10). The new equation

$$\boldsymbol{F}_1(\boldsymbol{a},x)\boldsymbol{a}' + \boldsymbol{G}_1(\boldsymbol{a},x) = 0 \tag{5.11}$$

would have had the same form as (5.10), but the last row of the matrices $\boldsymbol{F}_1$ and $\boldsymbol{G}_1$ would have been different from the lastrow of $\boldsymbol{F}$ and $\boldsymbol{G}$, so the singularity $\det \boldsymbol{F}_1 = 0$ would have occurred in a different point of phase space. The solution of the system (5.11) would have been close to the solution of (5.10) as long as both systems were far from the singularity $\det \boldsymbol{F} = 0$ and $\det \boldsymbol{F}_1 = 0$. Intuitively, the system (5.11) is as correct as (5.10). However, a solution cannot satisfy both (5.11) and (5.10), since in this case the system becomes over-constrained: there are more equations than unknowns.

Suppose we want to find a solution which satisfies both (5.10) and (5.11), i.e., a system of $N+1$ equations and $N$ unknowns, since the first $N-1$ equations of (5.10) and (5.11) are the same and only the last equation is different. More generally, we can consider a system of $L > N$ equations with $N$ unknowns, where the $m$-th equation is an averaged equation of the type (5.9). We define $L$ functions

$$E_m(\boldsymbol{a},\boldsymbol{a}',x) = \sum_{i=1}^{n} F_{im}(\boldsymbol{a},x)\boldsymbol{a}_i'(r) + G_m(\boldsymbol{a},x). \tag{5.12}$$

In principle, one should require that all the functions $E_m$, $1 \le m \le L$ are zero. However, this is impossible to achieve, since we only have $N$ unknowns $a_0(x), \ldots, a_{N-1}(x)$. Instead, we require that the functions $E_m$ are small 'on average'. More precisely, we define the error functional

$$\mathcal{E}[\boldsymbol{a}] = \int_{x_0}^{x_1} \sum_{m=1}^{L} E_m^2(\boldsymbol{a},\boldsymbol{a}',x)\mathrm{d}x \tag{5.13}$$

and impose the condition that $\boldsymbol{a}$ minimises the functional (5.13):

$$\delta\mathcal{E}[\boldsymbol{a}] = 0. \tag{5.14}$$

The condition (5.14) allows to write a well-determined set of differential equations for the unknowns $\boldsymbol{a}$. What is even more important, the resulting equation for $\boldsymbol{a}$ is non-singular. In fact, the calculating the $m$-th equation of (5.14) explicitly, we get:

$$\sum_k A_{mk}(\boldsymbol{a},\boldsymbol{a}',x)a_k'' + B_m(\boldsymbol{a},\boldsymbol{a}',x) = 0. \tag{5.15}$$

where $A_{mk} = \sum F_{mi}F_{ik}$ and $B_m$ are functions depending on $\boldsymbol{a}$, $\boldsymbol{a}'$ and $x$, but not on $\boldsymbol{a}''$. The singularity appears when $\det A = 0$. $A$ is an $N \times N$ matrix, and $F$ is an $N \times L$ matrix with $L > N$. If $F$ is $N \times N$ matrix, we have exactly as many equations as unknowns, $\det A = (\det F)^2$, and $A$ becomes singular at the same point as the solution to equation (5.10). This is very natural, because in the case $L = N$ the variational problem (5.14) has an exact solution, namely, $\boldsymbol{a}$ satisfying (5.10). In this case we also have $\mathcal{E} = 0$ on the solution. However, if $L > N$, it is much more difficult for $\det A$ to become 0, as we shall see immediately below. We shall consider the case $L = 3, N = 2$, which we have used in our calculations. In this case, the determinant of the matrix $A$ can be computed exactly:

$$\begin{aligned} detA = \textstyle\sum_i (\det M_i)^2 = (F_{11}F_{22} - F_{21}F_{22})^2 + \\ (F_{12}F_{23} - F_{23}F_{22})^2 + (F_{11}F_{23} - F_{13}F_{31})^2. \end{aligned} \tag{5.16}$$

We can see that $\det A$ is the sum of the squares of the determinants of the $2\times 2$ submatrices $M_i$, chosen within a $2 \times 3$ matrix $F$. We conjecture that a similar result holds for general $N$ and $L$, but we have been unable to prove it rigorously.

Due to (5.16), $\det A$ becomes 0 if and only if the determinants of all the submatrices $M_i$ vanish. In the case $L = 3$, $N = 2$ this will require 3 conditions to be satisfied. Since the dimension of the phase space is 2, it is in general impossible for the determinant of the matrix $A$ to vanish, and the system (5.15) never becomes singular.

First, we apply these ideas to the study of a flow in a flat pipe, corresponding to $h(x) \equiv 1$ in figure 5.1. The flow in such a channel is given by the parabolic profile for the velocity $u = 3/2(1-y^2)$, which corresponds to the streamfunction $\psi = 3/2(y-y^3/3)$. The flow is normalised in such a way that $\psi(\pm 1) = \pm 1$. We shall investigate to see if there could be an asymmetric solution in such a channel with the help of the minimal error method.

We assume a solution of the form:

$$\psi = \frac{3}{2}\left(y - \frac{y^3}{3}\right) + a(x)y^2(1-y^2). \tag{5.17}$$

Here $a(x)$ is the amplitude of an asymmetric perturbation in the velocity $u$, corresponding to a symmetric perturbation in $\psi$. We take the averaged momentum equation to be the first equation of our system. The second equation is the momentum equation, multiplied by $y$ and integrated from $-1$ to 1:

$$\begin{aligned} E_1(x) &= \tfrac{6400}{3773} a(x) a'(x) \\ E_2(x) &= \tfrac{16}{7} a(x)^2 + \tfrac{1829}{735} a'(x) \end{aligned} \tag{5.18}$$

The error functional for this system is

$$\mathcal{E} = \int_x \left(E_1(x)^2 + E_2(x)^2\right) \mathrm{d}x \tag{5.19}$$

One can identify the function under the integral in (5.19) as a Lagrangian. Equation (5.14) then corresponds to the minimum action principle of Hamiltonian dynamics. By making the Legendre transform, we obtain the Hamiltonian formulation for the variational problem $\delta\mathcal{E} = 0$ with $\mathcal{E}$ given by (5.19). The Hamiltonian is:

$$H(a,p) = \frac{15}{196R^2} \frac{10463113815p^2R^2 - 238050583232apR - -629145600000a^4}{19833933889 + 9216000000a^2}, \tag{5.20}$$

where the 'momentum' $p$ equals

$$p = \frac{58528}{5145R} a(x) + \frac{669048}{540225} a'(x) + \frac{81920000}{14235529} a(x)^2 a'(x) \tag{5.21}$$

We have used the package *Mathematica* to calculate (5.20-5.21). The evolution of $a(x)$ and $p(x)$ is then described by the equations:

$$\begin{aligned} p'(x) &= \frac{\partial H}{\partial a} \\ a'(x) &= -\frac{\partial H}{\partial p}. \end{aligned} \tag{5.22}$$

The fixed points of the system (5.22) are found by setting the right-hand sides of (5.22) to zero. We see that (5.22) has only one fixed point $a = p = 0$.

A physically meaningful solution of the system (5.22) has $a(x) \to 0, p(x) \to 0$ when $x \to \pm\infty$. Such a solution is a separatrix of the system (5.22), starting and ending at the fixed point $a = p = 0$. However, a separatrix for the Hamiltonian system (5.22) cannot exist due to the index theorem. The phase space is two-dimensional, and if there were a separatrix, it would have to encircle a fixed point [4]. However, $a = 0, p = 0$ is the only fixed point, as we have seen. Thus, for a flat pipe, the one-parameter approximation (5.17) only admits a parabolic velocity profile as a solution.

We shall now describe in more detail how the system (5.14) is solved for the case of an expanding channel with varying height $h(x)$. We shall use the same shape of channel as [1] in order to make a comparison with their results:

$$h(x) = \begin{cases} D, & |x| > 2 \\ D - \frac{D-1}{2}\cos(\pi x/2), & |x| < 2. \end{cases} \tag{5.23}$$

Height (5.23) specifies a channel of the type illustrated in figure 5.1. In what follows, we shall take $D = 3$. For (5.23), the derivative $h'(x)$ is continuous, but $h''(x)$ is discontinuous. We have also repeated our calculations for the smoothed boundary

$$h(x) = 1 + 2\tanh(50(1 - \cos(2\pi x/L))). \tag{5.24}$$

Here $L$ is the length of the channel and $h(x)$ is periodic with period $L$. The difference between $h(x)$, specified by (5.24) and (5.23), is very small, but (5.24) is infinitely smooth. We have found, as expected, that the results afforded by (5.24) and (5.23) are almost identical, so the discontinuity of $h''(x)$ does not play an essential role.

As we have mentioned, we have used the case $L = 3$ and $N = 2$ (three equations with two unknowns). In principle, one could solve the equations (5.15) as a boundary-value problem on the interval $x \in [x_0, x_1]$, say, with periodic boundary conditions or by requiring that the velocity profile is parabolic at $x = x_0$ and $x = x_1$. Equations (5.15) specify a boundary value problem for the coefficients $a_i$. We have, however, found out that the practical implementation of such a straightforward method is very difficult. A very accurate initial approximation to the solution is required for the convergence of a Newton iteration. A much simpler approach to this problem is to write the variation problem $\delta\mathcal{E} = 0$ as an evolution equation for $\boldsymbol{a}$ using the relaxation method:

$$\boldsymbol{a}_t = -\frac{\delta\mathcal{E}}{\delta\boldsymbol{a}}. \tag{5.25}$$

In this case, the fixed point $\boldsymbol{a}_t = 0$ corresponds to the minimum of the function $\mathcal{E}$. If we start with some arbitrary initial conditions $\boldsymbol{a}(x, t = 0)$, the solution $\boldsymbol{a}(x, t)$ quickly converges to the fixed point of (5.25), corresponding to the minimum of $\mathcal{E}$.

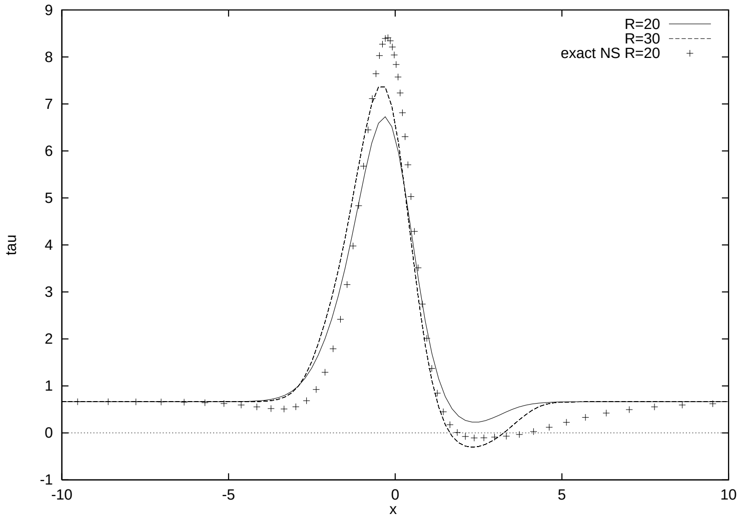


Figure 5.2: The shear stress $\tau$ on the bottom $y = -h(x)$ obtained by solving (5.25) for the two-mode model, with two values of Reynolds number the $R = 20$ and $R = 30$ (solid and dashed lines). For comparison, the shear stress from an exact numerical solution for $R = 20$ is also plotted (crosses) (courtesy of K. H. Andersen).

We have used the following ansatz:

$$\psi = \frac{3}{2}(\eta - \eta^3/3) + a_1(x)(1-\eta^2)^2 + a_2(x)\eta(1-\eta^2)^2. \tag{5.26}$$

In (5.26), $a_1 \equiv 0$ corresponds to the symmetric velocity profiles. The results of simulations are presented in figure 5.2. The shear stress $\tau(x) = u_y(x, y = -h(x))$ at the bottom is plotted for different values of the Reynolds numbers. We see that the separation occurs at $R \simeq 25$. The model encountered no problem when describing the flow with a separation of the boundary layer. The results of the simulations of the full Navier-Stokes equations (performed by K. H. Andersen) are also shown on the same figure. The separation of the boundary layer for the exact solution occurs for lower values of the Reynolds number as compared to the error minimisation method (the exact solution for $R = 20$ is already separated). The length of the separation bubble is underestimated, and the drop in shear stress *before* the contracting part of the channel is not predicted by our model. The maximum amplitude of the shear stress for our model is less than for the exact solution. We should also say that the agreement between the minimal error method and the exact solution becomes worse when the Reynolds number $R$ increases.

We note that we have not managed to observe the symmetry-breaking bifurcation for this model. The asymmetric velocity mode $a_1$ always converged to 0 even if we impose it to be non-zero in the initial conditions. We do not know whether this is due to some essential properties of the model which rule out the bifurcation, or whether this is just due to the fact that the symmetric state is always attractive in the sense of (5.25). This is not in contradiction with the results of [1], since the evolution equation (5.25) does not describe the real evolution in time, but is a 'fictitious' differential equation designed to help the functional $\mathcal{E}$ reach the minimum.

In conclusion, one can say that the minimal error principle (5.25) provides a simple and reliable method for obtaining the symmetric solution for the two-dimensional channel flow. The drawbacks of this method are:

1. If the number of unknowns $N$ or equations $L$ is large, the formulas (5.10) become algebraically tremendously complicated and their analytic investigation becomes difficult.

2. The symmetry-breaking bifurcation structure has not been observed. It could be that a larger number of unknowns $N$ and equations $L$ is necessary for the model (5.14) to describe the symmetry-breaking bifurcation. It could also be that the asymmetric solutions cannot be obtained by the minimal error method. Further studies of the problem are needed.

## 5.4 Extended Boundary-Layer Theory

We have seen that the integral methods remove the singularity of the boundary layer equations at the separation, but become singular at a different point of the phase space (like $\Lambda = 0$ in (2.42)). One way to get rid of these artificial singularities is the minimal error method described above. However, the minimal error method is in a way just a mathematical trick, which does not address the physical essence of the singularity. The singularity in the boundary layer equations at the separation, as we have emphasized, comes from the fact that the boundary layer approximation breaks down at the point of separation. Thus, a more consistent way to remove the singularity, exhibited by the boundary layer equations at the separation, is to take into account the terms neglected in the boundary layer approximation. Of course, if we include *all* the neglected terms, we would get back to the full Navier Stokes equations, which are not singular at the separation point (for a mathematically rigorous discussion of the Navier-Stokes equations, see [5]). It is thus best to stop half-way: only the relevant terms should be included, so the equations will still be simple enough to treat, but will not develop a singularity at the separation. We shall now return to chapter 1 and take a closer look at equation (1.15), which was the starting point of the boundary layer approximation.

The boundary layer approximations were obtained by neglecting terms of order $R^{-1}$ and higher in (1.15). It is reasonable to start by additionally including only terms of order $R^{-1}$ and neglecting the $O(R^{-2})$ terms. (The reader might be a little confused by this statement. One could consider the neglected terms as a perturbation of the boundary layer equations. This perturbation will be *singular*, and one would expect that it is reasonable to include the most singular terms $O(R^{-2})$ first. This is a complicated question, and we shall avoid discussing it. Our goal at this point is not to be rigorous, but rather to find a simple and effective cure to the boundary layer equations.)

The question is whether one has to include all the terms of order $R^{-1}$. For the reader's convenience, we shall list all the terms of order $R^{-1}$ in (1.15):

1. In the $X$ momentum equation (1.15.1) : the term $U_{XX}$ on the right-hand side.

2. In the $Y$ momentum equation (1.15.2): the terms on the left-hand side and the term $W_{YY}$ on the right-hand side.

Suppose we include all the terms listed above. In this case, the extended boundary layer approximation to (1.15) is:

$$
\begin{aligned}
&UU_X + WU_Y = -P_X + R^{-1}U_{XX} + U_{YY}\\
&R^{-1}(UW_X + WW_Y) = -P_Y + R^{-1}W_{YY}\\
&U_X + W_Y = 0,
\end{aligned}
\tag{5.27}
$$

and we have assumed the flow to be stationary. System (5.27) approximates (1.15) with an accuracy $O(R^{-2})$. However, one can easily see that the system (5.27) has a singularity at the separation and is thus not suitable for our purposes. To show this, we remove the pressure by taking the curl of the momentum equations (5.27.1-2), and use the stream-function $\psi$ with $u = \psi_Y, w = -\psi_X$. Suppose for the moment that $Y = 0$ corresponds to the solid surface (which was the convention in chapter 1). We expand $\psi$ as a power series in $Y$ around $Y = 0$

$$
\psi = \sum_{k\geq 2} a_k(X)Y^k \tag{5.28}
$$

and substitute into (5.27). In an analogous manner to the derivation of (1.35), at the order $Y^2$, we get

$$
a_2(X)a_2'''(X) = \text{Right-hand side.} \tag{5.29}
$$

Thus, $a_2(X)$ approaches the separation point $a_2 = 0$ as $a_2 \sim (X_* - X)^{3/2}$.

It might seem that the inclusion of the higher-order terms in the boundary layer equations leads to a dead end. In fact, the only term omitted in (5.27) is the term $R^{-2}W_{XX}$ on the right-hand side of the $Y$-momentum equation (1.15.2). But if we include this term also, we come back to the full Navier-Stokes equations!

The trick is to include only terms of order $1/R$ linear in the velocity and to drop the nonlinear terms on the left-hand side of (5.27.2):

$$
\begin{aligned}
&UU_X + WU_Y = -P_X + R^{-1}U_{XX} + U_{YY}\\
&0 = -P_Y + R^{-1}W_{YY}\\
&U_X + W_Y = 0.
\end{aligned}
\tag{5.30}
$$

The system (5.30) does not exhibit any singularity at the separation point, and we shall use it to compute the flow in the two-dimensional channel. We do not have an explanation why only these terms have to be taken into account.

Truncating the system (5.2) as in (5.30) corresponds to keeping the following terms:

$$
\begin{aligned}
&u_t + uu_x + wu_y = -p_x + \frac{1}{R}\Delta u\\
&0 = -p_y + \frac{1}{R}w_{yy}\\
&u_x + w_y = 0.
\end{aligned}
\tag{5.31}
$$

Correspondingly, the streamfunction equation (5.6) simplifies to:

$$\Delta\psi_t + \partial_y(\psi_y\psi_{xy} - \psi_x\psi_{yy}) = \frac{1}{R}\psi_{yyyy} + \frac{2}{R}\psi_{xxyy}. \tag{5.32}$$

We shall further simplify (5.32) by writing $\Delta\psi_t \simeq \psi_{yyt}$ which corresponds to the boundary layer approximation. Finally, our extended boundary layer equation, which defines the evolution of the streamfunction, is:

$$\psi_{yyt} + \partial_y(\psi_y\psi_{xy} - \psi_x\psi_{yy}) = \frac{1}{R}\psi_{yyyy} + \frac{2}{R}\psi_{xxyy}. \tag{5.33}$$

We rescale $y$ as $\eta = y/h(x)$ in (5.33). After this substitution, derivatives of $h(x)$ appear in (5.33). We only include the term $2h'(x)/h(x)\psi_\eta\psi_{\eta\eta}$ in the left hand side of (5.33). We have observed that the inclusion of the other terms containing the derivatives of $h$ does not change the result substantially, as long as the channel height $h(x)$ varies sufficiently smoothly. The resulting equation for the streamfunction $\psi$ is then

$$h(x)^2\psi_{\eta\eta t} + h(x)\partial_\eta(\psi_\eta\psi_{x\eta} - \psi_x\psi_{\eta\eta}) + 2\frac{h'(x)}{h(x)}\psi_\eta\psi_{\eta\eta} = \frac{1}{R}\psi_{\eta\eta\eta\eta} + \frac{2}{R}h(x)^2\psi_{xx\eta\eta}. \tag{5.34}$$

It is convenient to make the following substitution:

$$\psi(x,\eta) = \psi_0(\eta) + \phi(t,x,\eta), \tag{5.35}$$

where

$$\psi_0(\eta) = 3/2(\eta - \eta^3/3) \tag{5.36}$$

which corresponds to the parabolic velocity profile. Inserting (5.35) into (5.34), we get the following equation for $\phi$:

$$\begin{aligned} &\phi_{\eta\eta t}h(x)^2 + h(x)(U_0(\eta)\phi_{x\eta\eta} + \psi_0''(\eta)\phi_{x\eta} + \psi_0'''(\eta)\phi_x + \phi_\eta\phi_{x\eta\eta} - \phi_x\phi_{\eta\eta\eta}) = \\ &\frac{1}{R}\phi_{\eta\eta\eta\eta} + \frac{2}{R}h(x)^2\phi_{xx\eta\eta} - 2\frac{h'(x)}{h(x)}\psi_0'(\eta)\psi_0''(\eta). \end{aligned} \tag{5.37}$$

Integral methods are now used for solving (5.37). We approximate $\phi(x,\eta,t)$ by a sum of $N$ basis functions $\phi(x,\eta) = \sum_k a_k(t,x)P_k(\eta)$. The boundary conditions for the function $\phi(x,\eta)$ are

$$\phi(\eta = \pm 1) = \phi_\eta(\eta = \pm 1) = 0, \tag{5.38}$$

therefore, the functions $P_k(y)$ have to satisfy the boundary conditions:

$$\begin{aligned} &P_k(\pm 1) = 0 \\ &P_k'(\pm 1) = 0 \end{aligned} \tag{5.39}$$

with $P_k(-\eta) = P_k(\eta)$ if $k = 2m$, and $P_k(-\eta) = -P_k(\eta)$ if $k = 2m-1$. We choose these basis functions $P_k(\eta)$ to be orthogonal polynomials. We started with the system of polynomials

$$\begin{aligned} P_k(\eta) = \eta^{2k+2} - \frac{3k-1}{k-1}\eta^{2k} + \frac{3k+1}{k-1}\eta^{2k-2} - \frac{k+1}{k-1}\eta^{2k-4}, &\quad k \text{ even} \\ P_k(\eta) = \eta^k(1-\eta^2)^2, &\quad k \text{ odd}, \end{aligned} \tag{5.40}$$

and orthogonalised the basis (5.40) using the Gramm-Schmidt procedure. We have found that the orthogonality of the basis improves the result of the computations.

We have to specify $N$ equations for $N$ unknown functions $a_1(x,t),\ldots,a_N(x,t)$. We multiply equations (5.37) by $N$ different weight functions $I_i(\eta)$ (we have used $I_i(\eta) = P_i(\eta)$) and integrate from $-1$ to 1. The $i$th equation then reads:

$$\begin{aligned} &h(x)^2 A_{ij} a_{j,t} + \frac{1}{R} B_{ij} a_j + h(x) C_{ij} a_{j,x} + h(x) D_{ijk} a_j a_k + \\ &h(x) E_{ijk} a_j a_{k,x} = \frac{2}{R} h(x)^2 A_{ij} a_{xx} + \frac{2h'(x)}{h(x)} F_i, \end{aligned} \tag{5.41}$$

and the summation is assumed over the repeated indices $j$ and $k$. The coefficients $A, B, C, D, E, F$ are given by:

$$\begin{aligned} A_{ij} &= \textstyle\int_{-1}^{1} I_i(\eta) P_j''(\eta) \mathrm{d}\eta \\ B_{ij} &= -\textstyle\int_{-1}^{1} I_i(\eta) P_j''''(\eta) \mathrm{d}\eta \\ C_{ij} &= \textstyle\int_{-1}^{1} I_i(\eta) \left\{ \psi_0'(\eta) P_j''(\eta) + \psi_0''(\eta) P_j'(\eta) + \psi_0'''(\eta) P_j(\eta) \right\} \mathrm{d}\eta \\ D_{ijk} &= \textstyle\int_{-1}^{1} I_i(\eta) P_j'(\eta) P_k''(\eta) \mathrm{d}\eta \\ E_{ijk} &= \textstyle\int_{-1}^{1} I_i(\eta) P_j(\eta) P_k'''(\eta) \mathrm{d}\eta \\ F_i &= \textstyle\int_{-1}^{1} I_i(\eta) \psi_0''(\eta) \psi_0'''(\eta) \mathrm{d}\eta. \end{aligned} \tag{5.42}$$

Equations (5.41) are well-posed if the matrix $A$ is non-degenerate. This is determined by the choice of weight functions $I_i$ and is true for $I_i(\eta) = P_i(\eta)$. Multiplying (5.41) by the inverse of the matrix $A$ gives a nonlinear forced heat-conduction equation.

In the system (5.41), the equations for the even and odd modes in the velocity can be separated. Assume, for simplicity, that the number of modes $N$ is even. If we denote the odd modes in $\phi$ as $\Omega = (a_1, a_3, \ldots, a_{N-1})$ and the even modes as $\Theta = (a_2, a_4, \ldots, -a_N)$, the system (5.41) can be written symbolically as:

$$\begin{aligned} &\Omega_t + \mathcal{L}(\Omega) + \mathcal{B}_1(\Omega,\Omega) + \mathcal{B}_2(\Theta,\Theta) = \frac{2}{R}\Omega_{xx} + 2h'(x)/h(x)\tilde{F} \\ &\Theta_t + \mathcal{B}_1(\Theta,\Omega) = \frac{2}{R}\Theta_{xx}, \end{aligned} \tag{5.43}$$

where $\mathcal{L}$ is a linear operator, $\mathcal{B}_1$ and $\mathcal{B}_2$ are bilinear operators of both arguments, and the forcing is $\tilde{F} = A^{-1}F$. One can see that $\Theta = 0$ is always a solution of (5.43), but it can be unstable if $R$ is large enough. If $h'(x) = 0$ identically, the symmetric solution is the trivial $\Omega = 0$, since the forcing on the right-hand side of (5.43.1) vanishes. If $h'(x)$ is not identically zero, at some large enough value of $R$ the symmetric solution bifurcates and a solution with $\Theta \neq 0$ can appear. The point of bifurcation has to be determined numerically.

Following [1], we define the *asymmetry parameter* $\zeta$ as

$$\zeta^2 = \frac{\int (\Psi(x,y) - \Psi(x,-y))^2 \mathrm{d}x\mathrm{d}y}{\int \mathrm{d}x\mathrm{d}y}. \tag{5.44}$$

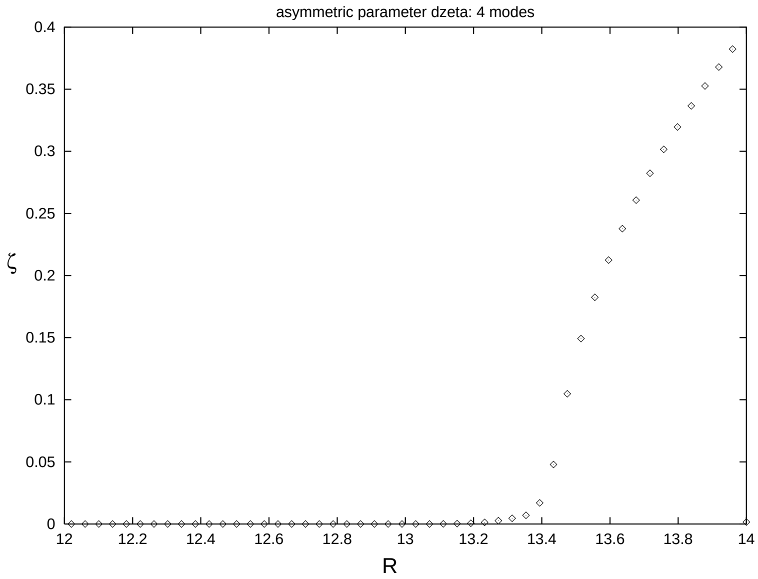


Figure 5.3: The asymmetry parameter $\zeta$ versus the Reynolds number $R$

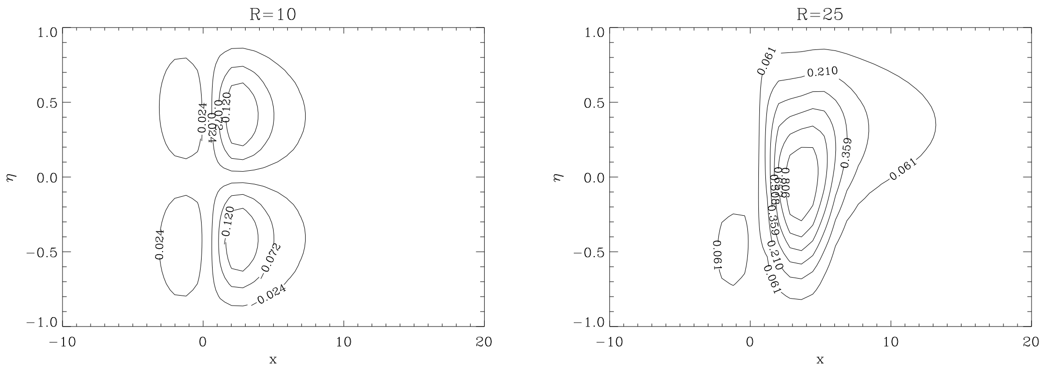


,

Figure 5.4: The streamlines of the converged solution for $R = 10$ and $R = 25$

One can see that $\zeta$ is just the $L_2$ norm of the asymmetric part $\Theta$. Thus, $\zeta = 0$ if and only if the velocity profile is symmetric and $\Theta \equiv 0$.

In our simulations, we have used $N = 4$ modes. In figure 5.3, we present the asymmetry parameter $\zeta$ versus $R$. The boundary conditions at the ends $x = x_0$ and $x = x_1$ were fixed to be $a_i = 0$, i.e., the profile was forced to be parabolic at both ends. Due to the orthonormality of the chosen basis functions, we have

$$\zeta^2 = \int \left\{ a_2(x)^2 + a_4(x)^2 \right\} \mathrm{d}x \tag{5.45}$$

The symmetry-breaking pitchfork bifurcation was observed to occur at $R \simeq 13.4$, which is in agreement with [1].

Finally, in figure 5.4 we present the contour plot of the solution $\phi(x, \eta)$, obtained by iterating (5.41) until convergence. The vertical coordinate is $\eta = y/h(x)$ and thus ranges from $-1$ to 1. The solution is symmetric for $R = 10$ but asymmetric for $R = 25$.

Unfortunately, the extended boundary layer model allows us only to predict the first symmetry-breaking bifurcation. We have failed to resolve the subsequent bifurcations observed in [1] when the value of $R$ was increased. Perhaps this is due to the fact that only 4 modes have been used in our computations, and by increasing the number of modes one might be able to achieve the resolution of the subsequent bifurcations as well. However, the computational time increases dramatically with the number of modes used. Therefore, we have not used more than 6 modes in our computations. We have observed that even a model with 6 modes could not resolve the subsequent bifurcations for the larger values of $R$.

However, there are still reasons to consider the model (5.37) and its approximation (5.41) as relative successes. The model (5.41) is quite simple and its computational implementation is straightforward and can be achieved even on a relatively small computer, at least for a small number of modes.

# Bibliography

[1] Sobey, I. J. & Drazin, P.G. (1986) *Bifurcations in two-dimensional channel flows J. Fluid Mech.*, **171**, 263.

[2] Borgas, M. S. & Pedley, T. J. (1990) *Non-uniqueness and bifurcations in annular and planar channel flows*, *J. Fluid Mech.*, **214** 229-250.

[3] Patterson, G. N., (1934) *Flow forms in a channel of small exponential divergence*, *Can. J. Res*, **11**, 770-779.

Patterson, G. N., (1935) *Viscosity effects in a channel of small exponential divergence*, *Can. J. Res*, **12**, 676-685.

[4] Lefschets, S. (1957). *Differential equations: Geometric theory*, Interscience, NY.

[5] Temam, R. (1997) *Navier-Stokes Equations*, North-Holland.